

This article was downloaded by: [National Chiao Tung University 國立交通大學]

On: 30 April 2014, At: 17:40

Publisher: Taylor & Francis

Informa Ltd Registered in England and Wales Registered Number: 1072954 Registered office: Mortimer House, 37-41 Mortimer Street, London W1T 3JH, UK



## Journal of the Air & Waste Management Association

Publication details, including instructions for authors and subscription information:  
<http://www.tandfonline.com/loi/uawm20>

### Silane Removal at Ambient Temperature by Using Alumina-Supported Metal Oxide Adsorbents

Jung-Nan Hsu<sup>b a</sup>, Chuen-Jinn Tsai<sup>b</sup>, Cindy Chiang<sup>b</sup> & Shou-Nan Li<sup>a</sup>

<sup>a</sup> Energy and Environment Research Laboratories, Industrial Technology and Research Institute, Hsinchu, Taiwan, Republic of China

<sup>b</sup> National Chiao Tung University, Institute of Environmental Engineering, Hsinchu, Taiwan, Republic of China

Published online: 29 Feb 2012.

To cite this article: Jung-Nan Hsu, Chuen-Jinn Tsai, Cindy Chiang & Shou-Nan Li (2007) Silane Removal at Ambient Temperature by Using Alumina-Supported Metal Oxide Adsorbents, *Journal of the Air & Waste Management Association*, 57:2, 204-210, DOI: [10.1080/10473289.2007.10465309](https://doi.org/10.1080/10473289.2007.10465309)

To link to this article: <http://dx.doi.org/10.1080/10473289.2007.10465309>

PLEASE SCROLL DOWN FOR ARTICLE

Taylor & Francis makes every effort to ensure the accuracy of all the information (the "Content") contained in the publications on our platform. However, Taylor & Francis, our agents, and our licensors make no representations or warranties whatsoever as to the accuracy, completeness, or suitability for any purpose of the Content. Any opinions and views expressed in this publication are the opinions and views of the authors, and are not the views of or endorsed by Taylor & Francis. The accuracy of the Content should not be relied upon and should be independently verified with primary sources of information. Taylor and Francis shall not be liable for any losses, actions, claims, proceedings, demands, costs, expenses, damages, and other liabilities whatsoever or howsoever caused arising directly or indirectly in connection with, in relation to or arising out of the use of the Content.

This article may be used for research, teaching, and private study purposes. Any substantial or systematic reproduction, redistribution, reselling, loan, sub-licensing, systematic supply, or distribution in any form to anyone is expressly forbidden. Terms & Conditions of access and use can be found at <http://www.tandfonline.com/page/terms-and-conditions>

# Silane Removal at Ambient Temperature by Using Alumina-Supported Metal Oxide Adsorbents

**Jung-Nan Hsu**

*Energy and Environment Research Laboratories, Industrial Technology and Research Institute, Hsinchu, Taiwan, Republic of China; and Institute of Environmental Engineering, National Chiao Tung University, Hsinchu, Taiwan, Republic of China*

**Chuen-Jinn Tsai and Cindy Chiang**

*Institute of Environmental Engineering, National Chiao Tung University, Hsinchu, Taiwan, Republic of China*

**Shou-Nan Li**

*Energy and Environment Research Laboratories, Industrial Technology and Research Institute, Hsinchu, Taiwan, Republic of China*

## ABSTRACT

Copper, zinc, and cerium oxide adsorbents supported on alumina were used to remove silane gas ( $\text{SiH}_4$ ). The adsorbents were prepared using a coprecipitation method and characterized by the inductively coupled plasma mass spectrometry, X-ray powder diffractometer, and Brunauer-Emmett-Teller method (BET). The silane removal efficiency and adsorption capacity of the adsorbents were investigated in this study. Test results showed that the adsorbents containing active species had a removal efficiency  $>99.9\%$  for  $\text{SiH}_4$  before breakthrough. Adsorbents containing mixed oxides ( $\text{CuO-CeO}_2/\text{Al}_2\text{O}_3$  and  $\text{CuO-ZnO}/\text{Al}_2\text{O}_3$ ), which showed well-dispersed active species and high BET surface areas, had a greater adsorption capacity than the adsorbents containing single metal oxide. However, when the  $\text{CuO-ZnO}/\text{Al}_2\text{O}_3$  adsorbents contain  $>40\%$  wt% of active metal oxides, the increase of active species lowered the BET surface area leading to a decrease of the adsorption capacity. Additionally, when the content of the active metal oxides was between 20% and 40%, the  $\text{CuO-ZnO}/\text{Al}_2\text{O}_3$  adsorbents demonstrated higher adsorption capacity.

## INTRODUCTION

Silane gas ( $\text{SiH}_4$ ) is widely used in the semiconductor industry in a variety of processes. It is often used to form

### IMPLICATIONS

Dry adsorption by metal oxides is a better way to remove silane when arsine coexists in the exhaust stream of the diffusion process of the semiconductor manufacturing plant. The best composition of the active component has to be determined to increase the adsorption capacity. This study shows that the copper oxide is a good active species for removing silane, and the addition of zinc oxide or cerium oxide enhances the adsorption capacity of the adsorbent substantially.

a layer of silicon dioxide ( $\text{SiO}_2$ ) in a chemical vapor deposition process. Used silane is then discharged as a residual gas into some point-of-use abatement systems. Silane is a pyrophoric gas, which spontaneously undergoes combustion in air with its concentration  $>1.4\%$ .

In the semiconductor industry, thermal oxidation and dry adsorption are the two common methods used for silane treatment. Both methods have good abatement efficiencies for silane.<sup>1,2</sup> Thermal oxidation type is more cost-effective for treating silane. However, dry adsorption is a preferred method for treating exhaust gases, which contain silane and arsine ( $\text{AsH}_3$ ) simultaneously.  $\text{AsH}_3$ , a highly toxic gas, will be converted to fine toxic  $\text{As}_2\text{O}_3$  particles by thermal oxidation. These fine toxic particles cannot be removed efficiently by the wet scrubber installed behind the thermal oxidizer and will be discharged into the ambient environment. Additionally, scrubbing water containing toxic arsenic particles must be treated by heavy metal removal process, which will increase the running cost. Therefore, dry adsorption is a preferred method under this circumstance.

Limited research has been reported in the literature on the dry adsorption of silane by metal oxides containing adsorbents. Some researchers studied the adsorption of toxic hydride gases, such as  $\text{AsH}_3$  and  $\text{pH}_3$ . Haacke et al.<sup>3</sup> found that activated carbon impregnated with copper and chromium is an effective medium to remove  $\text{AsH}_3$  from the effluent gas. They also showed that  $\text{AsH}_3$  was oxidized to  $\text{As}^0$ , whereas metal  $\text{Cu}^{2+}$ , coated on the activated carbon surface, was reduced to  $\text{Cu}^0$ . Subsequently,  $\text{As}^0$  and  $\text{Cu}^0$  were further oxidized to  $\text{As}^{+3}$  and  $\text{Cu}^{2+}$  when the adsorbent was exposed to air. Colabella et al.<sup>4</sup> indicated that  $\text{pH}_3$  adsorbed on the activated carbon would be oxidized to form  $\text{P}_2\text{O}_5$  or  $\text{P}_2\text{O}_3$  by introducing oxygen into the test system. Hardwick and Mailloux<sup>5</sup> treated  $\text{AsH}_3$  by using the Novapure S510 adsorbent (Novapure Corp.), which also contained copper. The result shows

that the S510 effectively removes  $\text{AsH}_3$  by chemical adsorption with a high adsorption capacity of 4.5 mol/L. Based on the literature, it is known that copper oxide is commonly used as the active species for removing hydride gases. However, adsorbents using activated carbon as the support, as shown in the literature,<sup>3,4</sup> are not safe for treating exhaust gases in the fab or sub-fab of the semiconductor industry because of their flammability.<sup>6</sup> Adsorbents of nonflammable support materials (e.g., metal oxides) are important, and the parameters influencing the adsorption capacity are also worth investigating.

Various sorption processes using the supported CuO adsorbents exist to remove the common air pollutants, such as  $\text{SO}_2$  and nitrogen oxides ( $\text{NO}_x$ ), from flue gas.<sup>7,8</sup> The preparation process of metal adsorbents is similar to that of metal catalysts, which requires high activity, sensitivity, and stability. The widely used preparation methods for metal catalysts are described with their merits and demerits by Pinna.<sup>9</sup> He suggested that the coprecipitation method is a preferred procedure for preparing supported catalysts with a metal loading >10–15% (wt/wt). ZnO is commonly added to  $\text{CuO}/\text{Al}_2\text{O}_3$  as a catalyst stabilizer,<sup>10</sup> which inhibits the formation of  $\text{CuAl}_2\text{O}_4$  and decreases the degree of crystallinity. El-Shobaky et al.<sup>10</sup> indicated that treatment of CuO with ZnO increased the specific surface area and total pore volume and hindered catalyst sintering. Recently,  $\text{CeO}_2$  was added to the  $\text{CuO}/\text{Al}_2\text{O}_3$  adsorbent/catalyst for simultaneous removal of  $\text{SO}_2$  and  $\text{NO}_x$  from stack gases.<sup>11</sup> An improvement of the simultaneous removal of  $\text{SO}_2$  and  $\text{NO}_x$  was investigated using cerium-copper oxide as a regenerative sorbent. The best sulfation performance was observed when the sorbent with a 1:1 molar ratio of cerium and copper was used.<sup>12</sup>

The objective of this study was to prepare and test the alumina-supported metal oxide adsorbents:  $\text{CuO}/\text{Al}_2\text{O}_3$ ,  $\text{ZnO}/\text{Al}_2\text{O}_3$ , and  $\text{CeO}_2/\text{Al}_2\text{O}_3$ . Adsorbents containing mixed active components,  $\text{CuO-ZnO}/\text{Al}_2\text{O}_3$  and  $\text{CuO-CeO}_2/\text{Al}_2\text{O}_3$ , were also prepared and tested for obtaining the optimized weight percent of the active species with a maximum adsorption capacity.

## EXPERIMENTAL WORK

### Sample Preparation

The adsorbents used in this study were prepared by the coprecipitation of metal precursors in aqueous solution of copper (II) nitrate-3-hydrate, zinc (II) nitrate-6-hydrate, cerium (III) nitrate-6-hydrate, and aluminum (III) nitrate-9-hydrate. The synthesis procedure includes dissolving all of the precursors in the deionized water, stirring at 300 rpm, and heating at 80 °C. Sodium carbonate was used to titrate the solution until its pH value reached ~6.8–7. After stirring the solution for 12 hr, the samples were then washed with deionized water, dried in air at 393 K for 12 hr, and calcined in air at 823 K for 6 hr.

According to the monolayer dispersion phenomena, ~40 wt% of CuO can be uniformly dispersed on the surface of  $\text{Al}_2\text{O}_3$  support, and the adsorption capacity would be maximum.<sup>13</sup> Based on the published result, the content of the active component was first chosen as 40 wt% (see Table 1). To further investigate the effect of the active component content on the adsorption capacity, several adsorbent batches of different weight percentages

**Table 1.** Compositions of the adsorbents with different contents of active metal oxides.

Sample No.	Composition of Active Oxides	CuO (wt%)	ZnO (wt%)	CeO <sub>2</sub> (wt%)	Al <sub>2</sub> O <sub>3</sub> (wt%)
1	CuO	40	0	0	60
2	CuO: ZnO = 2:1 <sup>a</sup>	27	13	0	60
3	CuO: ZnO = 1:1	20	20	0	60
4	ZnO	0	40	0	60
5	CeO <sub>2</sub>	0	0	40	60
6	CuO: CeO <sub>2</sub> =2:1	27	0	13	60
7	CuO: CeO <sub>2</sub> =1:1	20	0	20	60

Notes: <sup>a</sup>By weight percent.

with a fixed CuO-ZnO ratio (2:1) were used (refer to Table 2).

### Characterization of the Adsorbent

The metal contents of the adsorbents were analyzed by the inductively coupled plasma (ICP)-mass spectrometry (model Agilent 7500S, Agilent Technologies). Before analysis, the samples were pretreated by microwave digestion (MDS2000, CEM).

The surface area of the adsorbent was determined by the Brunauer-Emmett-Teller (BET) method applied to the adsorption isotherms of  $\text{N}_2$ , whereas the pore volume and the pore size distribution were determined by the Barret-Joyner-Halenda method applied to the desorption isotherms of  $\text{N}_2$ . Nitrogen adsorption/desorption isotherms were obtained by using an ASAP 2010 apparatus (Micromeritics Instrument Corp.).

The X-ray powder diffractometer (XRPD, model X-ray diffraction-6000, Shimadzu) was used to examine the crystalline structure of the adsorbents. The X-ray source used Cu as its target, and its working voltage and current were set at 40 kV and 30 mA, respectively. The scanning speed was 1°/min in the range of 5–90°.

The scanning electron microscopy ([SEM] model S4200, Hitachi) equipped with an energy-dispersive X-ray spectrometer ([EDS] model 432C-1ss, Noran Instrument) was used to obtain the micrographs and determine the elements on the adsorbent surface before and after the adsorption process. The acceleration voltage was 10 kV, and the amplification factor was 100 K.

The chemical states of compounds on the adsorbent surface were measured by the electron spectroscopy for chemical analysis ([ESCA] model ESCA Lab 250, Thermo

**Table 2.** Different active compound percentage of  $\text{CuO-ZnO}/\text{Al}_2\text{O}_3$  adsorbent with CuO wt%:ZnO wt% = 2:1.

Sample No.	Weight Percent of Active Oxides (%)	CuO (wt%)	ZnO (wt%)	Al <sub>2</sub> O <sub>3</sub> (wt%)
8	20	14	6	80
9	30	20	10	70
2	40	27	13	60
10	50	34	16	50
11	60	40	20	40
12	90	60	30	10

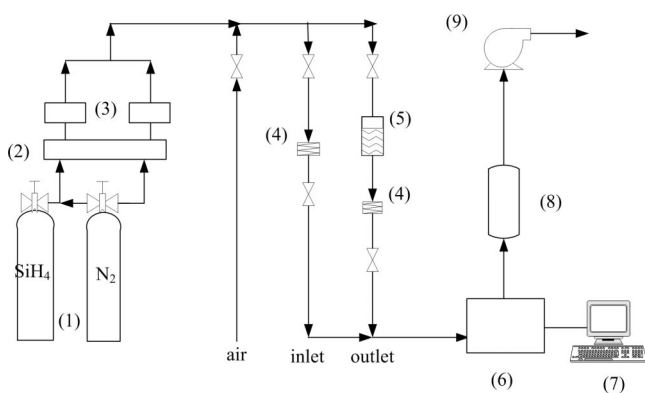


**Figure 1.** Schematic of the fixed-bed adsorption system. (1) SiH<sub>4</sub> and N<sub>2</sub> gas cylinder; (2) mass flow controller readout; (3) mass flow controller; (4) filter holder; (5) test chamber; (6) Fourier transform IR; (7) computer monitoring system; (8) dry scrubber; (9) vacuum pump.

Electron) before and after adsorption. The X-ray source used is Al K $\alpha$ . The binding energies determined in the experiments corresponded with the C 1s (1s orbital of carbon) value of 284.6 eV.

### Experimental Method for Testing SiH<sub>4</sub> Adsorption Capacity

A fixed-bed adsorption system, shown in Figure 1, was used to study the adsorption of SiH<sub>4</sub> gas at ambient temperature and pressure. The inlet concentration of SiH<sub>4</sub> was 1.2% (v/v), and the test gas flow rate was mostly 0.19 L/min. The cylindrical test chamber is made of stainless steel with an i.d. of 2.45 cm, packed with 30-cm<sup>3</sup> adsorbent. With the adsorption bed 6.1-cm long, the linear gas velocity is 0.67 cm/sec, and the residence time is 9.1 sec. To investigate the effect of linear gas velocity through the test bed on the adsorption capacity, the linear velocity was varied from ~0.33–1.63 cm/sec by adjusting the SiH<sub>4</sub> flow rate. The Fourier transform IR spectrometer (model I-2100, Midac) was used to measure the upstream and downstream silane concentration of the adsorption bed and to determine the adsorption efficiency and capacity of the adsorbents accordingly. A commercial dry adsorption barrel (model CV03S, CS), followed by an SiH<sub>4</sub> detector (model Polytron II, Drager), was installed at the end of the experimental system to treat the exhaust gas in the experimental system. This commercial adsorption device is normally used to treat the exhaust AsH<sub>3</sub> and pH<sub>3</sub> gases emitting from the implantation process of the semiconductor manufacturing plant.

The flow rate of the testing SiH<sub>4</sub> gas (1.2%, v/v) was adjusted using a mass flow controller. The flow rate, which was mostly 0.19 L/min, was checked before and after each SiH<sub>4</sub> adsorption testing by diluting the 1.2% SiH<sub>4</sub> gas with 99.999% nitrogen at a fixed flow rate ratio of 1:5 (SiH<sub>4</sub>:N<sub>2</sub>). The SiH<sub>4</sub> concentration after dilution was measured to be ~2000  $\pm$  110 ppm, which was very close to the theoretical concentration of 2000 ppm. The results demonstrated the flow and concentration accuracy of the test system. SiH<sub>4</sub> gas was found to be adsorbed on the adsorbents, and the outlet SiH<sub>4</sub> concentration remained almost zero until the adsorbents were almost spent. Thereafter, the outlet SiH<sub>4</sub> concentration started to increase. The time duration, when the outlet concentration

**Table 3.** Nominal and actual weight percentage of metal contents in the adsorbents.

Sample No.	Nominal			Actual		
	Cu (%)	Zn (%)	Ce (%)	Cu (%)	Zn (%)	Ce (%)
1	32	–	–	31.5	–	–
2	21.4	10.6	–	20.8	7.13	–
3	16	16	–	14.8	12.4	–
4	–	32	–	–	29.1	–
5	–	–	32	–	–	28.2
6	21.4	–	10.6	20.1	–	11.58
7	16	–	16	15.1	–	17.41

Notes: – = no data available.

was >10 ppm (or the removal efficiency [RE] <99.9%), was defined as breakthrough time in this study. The SiH<sub>4</sub> RE is defined as follows:

$$RE(\%) = [C_i - C_o]/C_i \times 100\% \quad (1)$$

where  $C_i$  is the influent SiH<sub>4</sub> volumetric concentration and  $C_o$  is the effluent SiH<sub>4</sub> volumetric concentration. The adsorption capacity can be based on moles ( $AC_m$ ) or weight of adsorbents ( $AC_w$ ), which are defined as follows:

$$AC_m (\text{mol SiH}_4/\text{mol MO}) = (Q \times C_i \times T/24.5)/Ma \quad (2)$$

$$AC_w (g\text{-SiH}_4/\text{kg-ads}) = (M_{\text{SiH}_4} \times Q \times C_i \times T/24.5)/W_{\text{ads}} \quad (3)$$

where  $MO$  represents all of the active metal oxides,  $Q$  (liters per minute) is the gas flow rate,  $C_i$  is the inlet SiH<sub>4</sub> volumetric concentration,  $T$  (minutes) is the breakthrough time,  $Ma$  (moles) is the number of moles of the active metal oxides used for testing,  $M_{\text{SiH}_4}$  is the molecular weight of SiH<sub>4</sub>, and  $W_{\text{ads}}$  (kilograms) is the weight of adsorbent used for testing.

The capacity depends on the type of the adsorbent used for adsorption. After the test, nitrogen gas was first blown through the pipes to remove the residual SiH<sub>4</sub> gas, and the clean purge air was then allowed to pass through the tubes for 120 min before the adsorbent was removed from the test bed for further analysis.

## RESULTS AND DISCUSSION

### Characteristics of the Adsorbent

The metal content of the adsorbents was measured by the ICP-mass spectrometry, and the results are shown in Table 3. The table shows that the actual metal amount of the product is close to the expected value (within  $\pm 10\%$  of the error for Cu,  $\pm 25\%$  for Zn, and  $\pm 12\%$  for Ce), which indicates that the current coprecipitation method is able to produce the adsorbents of the desired active components. Table 4 lists the BET surface area and the pore volume of the adsorbents shown in Table 1 (samples 1–7). It shows that all adsorbents with 40% (wt) of the active metal oxides have the BET surface areas >100 m<sup>2</sup>/g. The adsorbents containing mixed metal oxides have greater

**Table 4.** BET surface area and pore volume of the adsorbents containing different active metal oxides, which accounts for 40 wt% of the total weight.

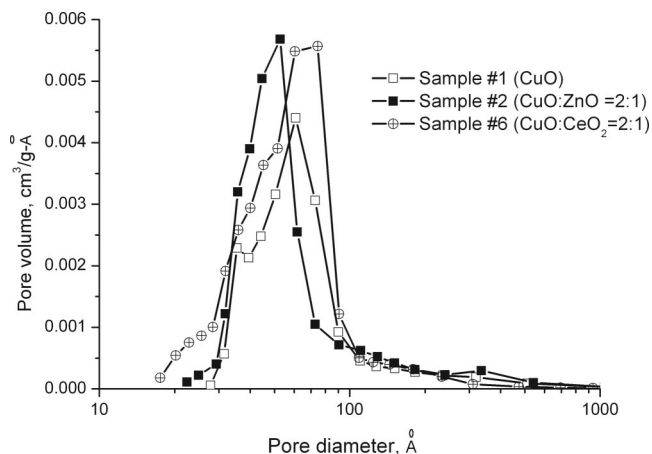
Sample No.	Composition of Active Oxides	Surface Area (m <sup>2</sup> /g)	Pore Volume (cm <sup>3</sup> /g)
1	CuO	121	0.297
2	CuO:ZnO = 2:1	148	0.323
3	CuO:ZnO = 1:1	139	0.384
4	ZnO	114	0.269
5	CeO <sub>2</sub>	100	0.234
6	CuO:CeO <sub>2</sub> = 2:1	154	0.349
7	CuO:CeO <sub>2</sub> = 1:1	152	0.256

BET surface areas and pore volumes than those of the adsorbents containing a single metal oxide. For example, the surface areas of samples 2 (CuO:ZnO = 2:1), 3 (CuO:ZnO = 1:1), 6 (CuO:CeO<sub>2</sub> = 2:1), and 7 (CuO:CeO<sub>2</sub> = 1:1), are 148, 139, 154, and 152 m<sup>2</sup>/g, respectively, which are larger than that of sample 1 (single oxide CuO) at 121 m<sup>2</sup>/g. When the total amount of active metal oxides (CuO and ZnO) increase from 20% to 90% (wt/wt), the surface area decreases from 156 to 42 m<sup>2</sup>/g, as shown in Table 5. The decrease is more obvious as the total weight percent increases from 40% to 90%. This finding is similar to that by Deng and Lin,<sup>7</sup> whose active species have a much smaller surface area. Such decrease in the surface area will lead to a sharp decrease in the adsorption capacity to be shown later. Figure 2 shows the pore distributions of samples 1 (CuO/Al<sub>2</sub>O<sub>3</sub>), 2 (CuO-ZnO/Al<sub>2</sub>O<sub>3</sub>), and 6 (CuO-CeO<sub>2</sub>/Al<sub>2</sub>O<sub>3</sub>). The pore volume peaks at the pore diameter of 40–80 Å, and the mixed CuO-ZnO (sample 2) adsorbent has more pore volume existing in the small pore size range than the single CuO (sample 1) adsorbent. However, the pore volume distribution of the mixed CuO-CeO<sub>2</sub> (sample 6) is quite similar to that of the CuO adsorbent (sample 1).

The XRPD patterns of adsorbents with different metal oxides (samples 1–7) are shown in Figure 3a. The single active metal oxide adsorbents are shown to have stronger XRPD peak intensity than those of the mixed oxides. For example, the adsorbent containing single active specie of 40% CuO (sample 1) shows narrow and strong diffraction peaks at 2θ = 35.6 and 38.8° (corresponding with the diffraction line of CuO crystallite). Similarly, sample 4 containing 40% ZnO shows sharp diffraction peaks at 31.8 and 34.8° (ZnO crystallite), and sample 5 shows

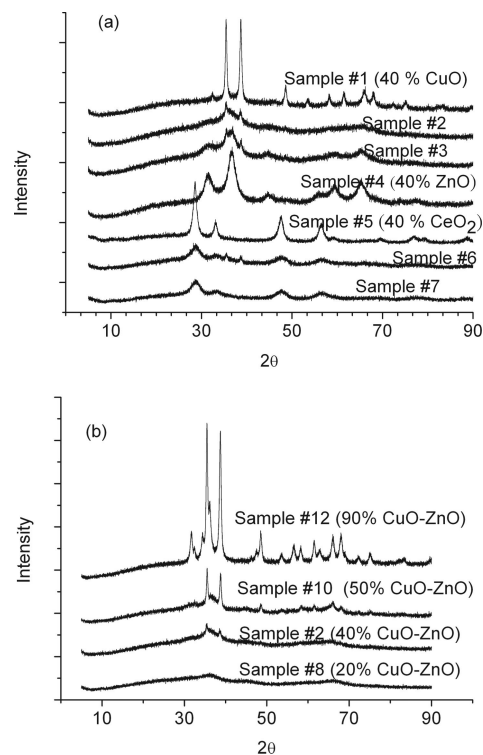
**Table 5.** BET surface area of the CuO-ZnO/Al<sub>2</sub>O<sub>3</sub> adsorbents with different weight percentages of active metal oxides.

Sample No.	Composition of Active Oxides	Total Weight Percent of Active Oxides (%)	Surface Area (m <sup>2</sup> /g)
8	CuO:ZnO = 2:1	20	156
9	CuO:ZnO = 2:1	30	146
2	CuO:ZnO = 2:1	40	148
10	CuO:ZnO = 2:1	50	120
11	CuO:ZnO = 2:1	60	87
12	CuO:ZnO = 2:1	90	42

**Figure 2.** Pore size distributions of the adsorbents.

sharp peaks at 28.5 and 47.4° (CeO<sub>2</sub> crystallite). In comparison, the broader and weaker XRPD peaks of adsorbents with mixed oxides suggest an amorphous-like phase or microcrystalline state. The results show that addition of Zn or Ce has a significant influence on the crystallite structure of the adsorbents. The mixed metal oxides can disperse well on the alumina to form a monolayer or submonolayer stable form.<sup>13</sup>

Figure 3b shows the XRPD pattern of CuO-ZnO/Al<sub>2</sub>O<sub>3</sub> adsorbents with different weight percentages of active components. The XRPD peak intensities of CuO crystallite appear to be present in the adsorbent with an active component loading >40%. The copper oxide and zinc oxide phases are present in an amorphous-like or

**Figure 3.** XRPD patterns of the adsorbents, (a) with 40% (by weight) of total active metal oxides, (b) with different total weight percents of active metal oxides; CuO:ZnO = 2:1 (by weight).

**Table 6.** Adsorption capacity of different active metal oxides with 40 wt% of total active metal oxides and linear gas velocity = 0.67 cm/sec.

Sample No.	Composition of Active Oxides	Adsorption Capacity (mol of SiH <sub>4</sub> /mol MO)	Adsorption Capacity (g SiH <sub>4</sub> /kg of adsorbent)
1	CuO	0.15	23.5
2	CuO:ZnO = 2:1	0.22 ± 0.015	35.7 ± 2.43
3	CuO:ZnO = 1:1	0.17	27.2
4	ZnO	0.11	17.7
5	CeO <sub>2</sub>	0.04	3.09
6	CuO:CeO <sub>2</sub> =2:1	0.25	33.4
7	CuO:CeO <sub>2</sub> =1:1	0.19 ± 0.023	22.7 ± 2.74

microcrystalline state when the weight percentage of the active metal oxides is <40%.

### Influence of Different Active Oxides on the Adsorption Capacity

The test results of the adsorption capacity for the adsorbents containing different active metal oxides are shown in Table 6. The linear SiH<sub>4</sub> gas velocity is 0.67 cm/sec, and the gas residence time in the adsorption bed is 9.1 sec. Before breakthrough, the outlet SiH<sub>4</sub> concentration is zero, which indicates the adsorbents having an adsorption efficiency of >99.9%. For the tested adsorbents of single active oxides, CuO/Al<sub>2</sub>O<sub>3</sub> has the highest adsorption capacity of 0.15 mol SiH<sub>4</sub>/mol of all active metal oxides (MO); CeO<sub>2</sub>/Al<sub>2</sub>O<sub>3</sub> adsorbent has the smallest capacity of 0.04 mol SiH<sub>4</sub>/mol MO. It appears that CeO<sub>2</sub> has the lowest activity for adsorbing SiH<sub>4</sub>, whereas CuO has the highest activity. Compared with single oxide adsorbents, adsorbents containing mixed oxides are shown to have a higher capacity. Such results can be inferred from the XRPD patterns shown in Figure 3a. The crystallinity of the single metal oxide adsorbents is clear, rather than the amorphous state of the mixed metal oxide adsorbents. This structural difference leads to a lower adsorption capacity for the single metal oxide adsorbent.

The addition of ZnO to CuO increases the BET surface area from 121 to 148 m<sup>2</sup>/g, and the adsorption capacity is increased from 0.15 to 0.22 mol SiH<sub>4</sub>/mol MO when the weight ratio of CuO:ZnO is 2:1. Adding more ZnO to CuO/Al<sub>2</sub>O<sub>3</sub> (CuO:ZnO = 1:1) lowers the adsorption capacity to 0.17 mol of SiH<sub>4</sub>/mol MO because of a lower BET surface area of 139 m<sup>2</sup>/g. Similarly, when CuO is mixed with CeO<sub>2</sub>, the adsorption capacity is also increased from

0.15 to 0.25 mol SiH<sub>4</sub>/mol MO for CuO:CeO<sub>2</sub> at 2:1 and from 0.15 to 0.19 mol SiH<sub>4</sub>/mol MO for CuO:CeO<sub>2</sub> at 1:1.

The adsorption capacity of CuO-CeO<sub>2</sub> and CuO-ZnO adsorbents is almost the same when the ratio of CuO:CeO<sub>2</sub> or CuO:ZnO is 2:1 (wt/wt). The CuO-ZnO adsorbent will be more cost effective than CuO-CeO<sub>2</sub> because of the much cheaper price of zinc/kg than that of cerium.

### Influence of Weight Percentages of Metal Oxides on the Adsorption Capacity

The test results for different weight percentages of CuO-ZnO are shown in Table 7. On a molar basis, the highest adsorption capacity of the adsorbent is at 0.23 mol SiH<sub>4</sub>/mol MO when the total CuO-ZnO is 30% by weight. However, on a mass basis, the adsorbent with 40% of CuO-ZnO has the highest adsorption capacity of 35.7 g SiH<sub>4</sub>/kg adsorbent because it contains more active components. To investigate the effects of active species (CuO and ZnO) content and BET surface areas on the SiH<sub>4</sub> adsorption capacity, test results are plotted in Figure 4 for illustration purposes. As Figure 4 shows, the adsorption capacities of adsorbents are similarly high when the weight percentage of active species (CuO-ZnO) is <40%, corresponding with the higher surface area. This is because of the well dispersion of the active species when the surface area of the adsorbent is large enough. However, if the amount of active oxides continuously increases, the BET surface area will decrease as shown in Table 5 because of the pore blockage in the alumina support. In addition, the crystals of the active oxides become larger (Figure 3b). These phenomena result in a sharp decrease of the adsorption capacity from 35.7 to 3.7 g SiH<sub>4</sub>/kg adsorbent when the CuO-ZnO is increased from 40% to 90%.

**Table 7.** Adsorption capacity of different weight percentages of the CuO-ZnO/Al<sub>2</sub>O<sub>3</sub> adsorbents with CuO:ZnO = 2: 1 (wt%).

Sample No.	Weight Percentage of Active Oxide	Adsorption Capacity (mol SiH <sub>4</sub> /mol MO)	Adsorption Capacity (g SiH <sub>4</sub> /kg adsorbent)
8	20	0.21 ± 0.017	17.1 ± 1.38
9	30	0.23	28.3
2	40	0.22 ± 0.015	35.7 ± 2.43
10	50	0.16	32.5
11	60	0.06 ± 0.009	13.9 ± 2.09
12	90	0.01	3.7

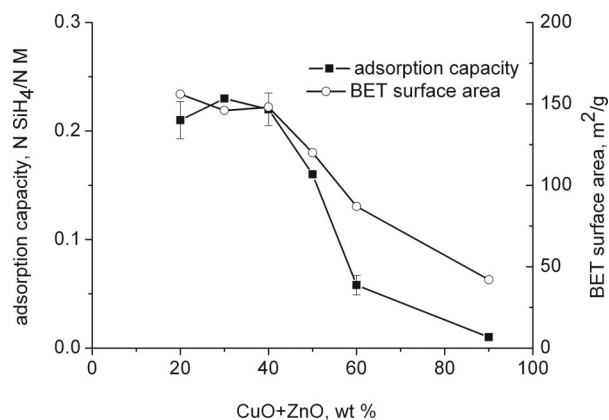


**Figure 4.** Relationship between adsorption capacity and BET surface area at different weight percentages of CuO-ZnO/Al<sub>2</sub>O<sub>3</sub> adsorbents.

### Influence of the Linear Gas Velocity on the Adsorption Capacity

The influence of the linear gas velocity on the adsorptive capacity was studied using the CuO-ZnO/Al<sub>2</sub>O<sub>3</sub> adsorbent with 40 wt% of CuO-ZnO (CuO:ZnO = 2:1). Different linear velocities were achieved by adjusting the flow rate of 1.2% SiH<sub>4</sub>. The operation conditions of this test and the results are summarized in Table 8. The data show that the adsorption capacity of the adsorbent increases from 14.8 to 37.7 g SiH<sub>4</sub>/kg adsorbent with decreasing linear velocity from 1.63 to 0.33 cm/sec. The adsorption capacity remains almost the same when the linear velocity of SiH<sub>4</sub> gas is <0.71 cm/sec. It indicates that SiH<sub>4</sub> gas has sufficient time to diffuse into the pores and becomes adsorbed on the adsorbent when the linear velocity of SiH<sub>4</sub> gas is <0.71 cm/sec. In comparison, the contact time is inadequate for SiH<sub>4</sub> to diffuse and to be adsorbed on the adsorbent when the gas linear velocity is >0.71 cm/sec. The data obtained in Table 8 are useful for scaling up the fixed-bed adsorbent for SiH<sub>4</sub> treatment.

### Surface Analysis of the Adsorbent

To understand the adsorption mechanism of SiH<sub>4</sub>, the surface analysis was conducted before and after the adsorption test. The typical SEM images of CuO-ZnO/Al<sub>2</sub>O<sub>3</sub> before and after adsorption are shown in Figure 5. The figures reveal that there are some spherical particles coagulating on the surface of the adsorbents after adsorption.

**Table 8.** Effect of different linear gas velocities on the adsorption capacity of the CuO-ZnO/Al<sub>2</sub>O<sub>3</sub> adsorbent.

Sample No.	Linear Velocity (cm/sec)	Adsorption Capacity (N of SiH <sub>4</sub> /N of MO)	Adsorption Capacity (g SiH <sub>4</sub> /kg adsorbent)
2-1	0.33	0.23	37.7
2-2	0.67	0.22 ± 0.015	35.7 ± 2.43
2-3	0.71	0.22	35.8
2-4	0.88	0.20	31.3
2-5	0.99	0.17	27.3
2-6	1.24	0.15	24.3
2-7	1.63	0.09	14.8

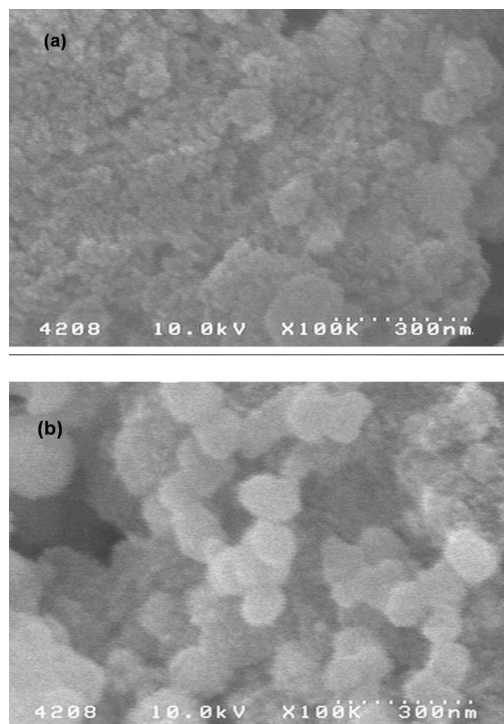


**Figure 5.** SEM images of CuO-ZnO/Al<sub>2</sub>O<sub>3</sub> adsorbents (a) before adsorption and (b) after adsorption.

From the EDS analysis, it is clear that some Si atoms are formed on the particle surface. It suggests that these particles may be made of Si, such as SiO<sub>2</sub>. The changes of the chemical states of Cu, Zn, and Al for CuO-ZnO/Al<sub>2</sub>O<sub>3</sub> adsorbents were measured by an ESCA before and after adsorption. Results show that there is no apparent change for the peak binding energy of the active components, such as Cu and Zn. However, an apparent change is observed at the binding energy peak of 101.9 eV (Figure 6). According to the reported data in the National Institute for Standards and Technology X-ray photoelectron spectroscopy database,<sup>14</sup> this binding energy can be assigned to the photoelectron at the 2p orbital of Si, of which the chemical state is in the form of SiO<sub>x</sub>, 0 < x < 2. Based on these results, the reaction between SiH<sub>4</sub> and CuO can be inferred to be similar to that among AsH<sub>3</sub>, PH<sub>3</sub>, and

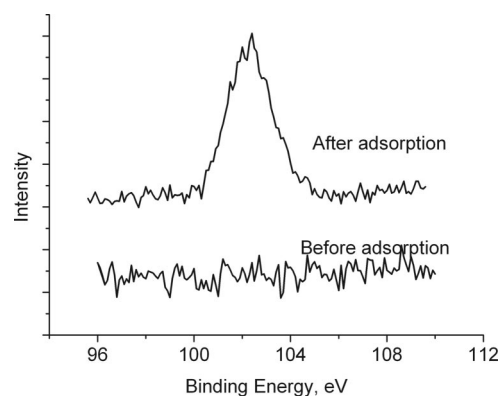


**Figure 6.** ESCA analysis of CuO-ZnO/Al<sub>2</sub>O<sub>3</sub> adsorbents before and after adsorption.

CuO.<sup>3,4</sup> The following reactions are proposed to take place during SiH<sub>4</sub> adsorption by CuO-ZnO/Al<sub>2</sub>O<sub>3</sub>:



The following reactions are proposed to take place after the adsorbent is exposed to air:



The results indicate that SiH<sub>4</sub> can be removed from the exhaust gas by reacting with the active species (CuO) of the adsorbents.

## CONCLUSIONS

In this study, dry adsorption of SiH<sub>4</sub> was studied using an alumina-supported adsorbent containing single-metal or mixed-metal oxides prepared by the coprecipitation method. The SiH<sub>4</sub> RE of all of the synthesized metal oxide adsorbents was found to be >99.9% before breakthrough. The adsorption capacity of the adsorbents containing mixed-metal oxides was found to be larger than that of the adsorbents containing a single active component, and the adsorption capacity was found to be in the following order: CuO-CeO<sub>2</sub>/Al<sub>2</sub>O<sub>3</sub> > CuO-ZnO/Al<sub>2</sub>O<sub>3</sub> > CuO/Al<sub>2</sub>O<sub>3</sub> > ZnO/Al<sub>2</sub>O<sub>3</sub> > CeO<sub>2</sub>/Al<sub>2</sub>O<sub>3</sub>. Higher adsorption capacity of the mixed oxide adsorbents was because of the amorphous structure of the active components rather than the crystalline structures of the single active component. The mixed-metal oxides were dispersed well on the alumina to form a monolayer or submonolayer form, which increased the adsorption capacity.

At a linear gas velocity of 0.67 cm/sec and a weight ratio of 2:1 for CuO/ZnO and CuO/CeO<sub>2</sub>, the adsorption capacity reached a maximum value of 0.22 mol SiH<sub>4</sub> per mol MO and 0.25 mol SiH<sub>4</sub>/mol MO, respectively. In addition, the CuO-ZnO/Al<sub>2</sub>O<sub>3</sub> adsorbent composed of 30% active metal oxides had the highest adsorption capacity (0.23 mol SiH<sub>4</sub>/mol MO) than CuO-ZnO/Al<sub>2</sub>O<sub>3</sub> adsorbents with lower or higher composition of active metal oxides. However, the decrease of BET surface area, which was caused by the increase of active metal oxides, results in a sharp decrease of adsorption capacity when the weight percent of active metal oxides was >40%.

In studying the effect of linear gas velocity on the SiH<sub>4</sub> adsorption capacity, it was found that the capacity remained almost the same when the linear velocity of the SiH<sub>4</sub> gas was <0.71 cm/sec. However, the adsorbent capacity decreased from 37.7 to 14.8 g of SiH<sub>4</sub>/kg adsorbent as the linear velocity increased from 0.33 to 1.63 cm/sec. That is, to effectively use the adsorbent, sufficient contact time was required for SiH<sub>4</sub> to diffuse and then be adsorbed on the adsorbent. These data are useful to the scale-up of the fixed-bed adsorbent system for SiH<sub>4</sub> removal.

Different from the published literature for treating hydride gases,<sup>4,5</sup> safer alumina-supported metal oxide adsorbents were used in this study. The preferred composition of metal oxides and the relevant parameters, such as

the linear gas velocity, for treating SiH<sub>4</sub> were obtained in this study, which could be used to maximize the adsorption capacity and minimize the waste adsorbent generated. However, this study was conducted only for removing SiH<sub>4</sub> in the exhaust gas. The optimum composition of metal oxides for treating other toxic hydrides, such as AsH<sub>3</sub> and PH<sub>3</sub>, and SiH<sub>4</sub> in the presence of other hydrides is worth investigating, and the study will be conducted in the future.

## REFERENCES

- Li, S.N.; Hsu, J.N.; Shih, H.Y.; Lin, S.J.; Hong, J.L. FTIR spectrometers measure scrubber abatement efficiencies. *Solid State Technol.* **2002**, *45*, 157-165.
- Hayes, M.; Woods, K. Treating Semiconductor Emissions with Point-of-Use Abatement System. *Solid State Technol.* **1996**, *39*, 141-146.
- Haacke, G.; Brinen, J.S.; Burkhard, H. Arsine Adsorption on Activated Carbon; *J. Electrochem. Soc.* **1988**, *3*, 715-717.
- Colabella, J.M.; Stall, R.A.; Sorenson, C.T. The Adsorption and Subsequent Oxidation of ASH<sub>3</sub> and PH<sub>3</sub> on Activated Carbon; *J. Cryst. Growth* **1988**, *92*, 189-195.
- Hardwick, S.J.; Mailloux, J.C. Waste Minimization in Semiconductor Processing; *Mat. Res. Soc. Symp. Proc.* **1994**, *344*, 273-279.
- Ogle, R.A.; Carpenter, A.R.; Morrison, D.T. Lessons Learned from Fires and Explosions Involving Air Pollution Control Systems; *Process Saf. Prog.* **2005**, *24*, 120-125.
- Deng, S.G.; Lin, Y.S. Synthesis, Stability, and Sulfation Properties of Sol-Gel-Derived Regenerative Sorbents for Flue Gas Desulfurization; *Ind. Eng. Chem. Res.* **1996**, *35*, 1429-1437.
- Yoo, K.S.; Kim, S.D.; Park, S.B. Sulfation of Al<sub>2</sub>O<sub>3</sub> in Flue Gas Desulfurization by CuO/T-Al<sub>2</sub>O<sub>3</sub> Sorbent; *Ind. Eng. Chem. Res.* **1994**, *33*, 1786-1791.
- Pinna, F. Supported Metal Catalysts Preparation; *Catalysis Today* **1998**, *41*, 129-137.
- El-Shobaky, G.A.; Fagal, G.A.; Mokhtar, M. Effect of ZnO on Surface and Catalytic Properties of CuO/Al<sub>2</sub>O<sub>3</sub> System; *Appl. Catal. A:Gen.* **1997**, *155*, 167-178.
- Akyurtlu, J.F.; Akyurtlu, A. Behavior of Ceria-Copper Oxide Sorbents under Sulfation Conditions; *Chem. Eng. Sci.* **1999**, *54*, 2991-2997.
- Wey, M.Y.; Lu, C.Y.; Tseng, H.H.; Fu, C.H. The Utilization of Catalyst Sorbent in Scrubbing Acid Gases from Incineration Flue Gas; *J. Air & Waste Manage. Assoc.* **2002**, *52*, 449-458.
- Xie, Y.C.; Tang, Y.Q. Spontaneous Monolayer Dispersion of Oxides and Salts onto Surfaces of Supports: Applications to Heterogeneous Catalysis; *Adv. Catal.* **1990**, *37*, 1-43.
- Aamink, W.A.M.; Weishaut, A.; Silfhout, A.V. Angle-Resolved X-Ray Photoelectron Spectroscopy and a Modified Levenberg-Marquardt Fit Procedure: A New Combination for Modeling Thin Layers; *Appl. Surf. Sci.* **1990**, *45*, 37-48.

### About the Authors

Jung-Nan Hsu is a Ph.D. student at the Institute of Environmental Engineering, National Chiao Tung University. He also works for the Industrial Technology and Research Institute, Taiwan. Chuen-Jinn Tsai is a professor at the Institute of Environmental Engineering, National Chiao Tung University. Shou-Nan Li is a manager of the Industrial Technology and Research Institute, Taiwan. Cindy Chiang is a graduate student at the Institute of Environmental Engineering, National Chiao Tung University. Address correspondence to: Chuen-Jinn Tsai, Institute of Environmental Engineering, National Chiao Tung University, Hsinchu 300, Taiwan, Republic of China; phone: +886-3-5731880; fax: +886-3-5727835; e-mail: cjtai@mail.nctu.edu.tw.